

Fundamental limitations to no-jerk gearshift in electric vehicles: the importance of transmission architectures

Marc-Antoine Beaudoin ^{*†} Benoit Boulet [†]

December 23, 2020

Abstract

Multi-speed transmissions can enhance the performance and reduce the overall cost of an electric vehicle, but they also introduce a challenge: avoiding gearshift jerk, which may sometimes prove to be impossible in the presence of motor and clutch saturation. In this article, we introduce three theorems that explicitly define the fundamental limitations to no-jerk gearshifts resulting from motor or actuator saturation. We compare gearshifts that consist of transferring transmission torque from one friction clutch to another, to the case in which one of the clutches is a one-way clutch. We show that systems with a one-way clutch are more prone to motor saturation, thus gearshift jerk is more often inevitable. We also study the influence of planetary gearsets on the gearshift dynamical trajectories, and expose the impact on the no-jerk limitations. This work offers tools to compare transmission architectures during the conceptual design phase of a new electric vehicle.

Keywords: electric vehicle, multi-speed transmission, transmission architecture, gearshift trajectory, gearshift jerk

1 Introduction

Uninterrupted gearshifts are a desirable feature of electric vehicles, but not all multi-speed transmissions are capable of it. To provide this capability, vehicle design engineers must select a transmission architecture where the motor torque can be continuously transferred from one transmission path to another during gearshifts. But in the presence of motor and clutch saturation, even these transmissions can fail to provide an uninterrupted gearshift. In this article, we explore the fundamental limitations on gearshift performance that originate from actuator saturation.

These fundamental limitations should be considered early in an electric vehicle design process, such as when selecting the transmission type during the conceptual design phase. Established design methodologies attribute a high importance to the conceptual design phase, as its outcome has a large influence on the rest of the design project, and ultimately, the product quality [1, 2, 3]. We wish to provide electric vehicle design engineers clear expectations on the potential gearshift performance of various transmission architectures, before they delve into resource-intensive detailed modelling.

^{*}Corresponding author: ma.beaudoin@mail.mcgill.ca

[†]Intelligent Automation Lab, McGill University, Room 503, McConnell Engineering Building, 3480 University Street, Montreal, QC, Canada, H3A 0E9

1.1 Review of powertrain architectures

The literature abounds with powertrain concepts, each with the potential to meet specific client needs [4, 5]. Perhaps the simplest architecture is using a single motor and a fixed reduction ratio between the motor and the wheels. This concept has an excellent drivability, but it introduces significant drawbacks on the vehicle design: to meet vehicular performance specifications, the motor is often oversized, and the resulting powertrain only seldom operates in its optimal efficiency region. This becomes especially problematic for heavier vehicles.

A natural evolution of the single-motor fixed-ratio concept is the introduction of a multi-speed transmission. A simple concept is the manual transmission [6, 7]. It consists of mounting gears on bearings, and selectively locking different gears to their transmission shafts to achieve different transmission ratios. Because electric motors do not need to idle, it is possible to use a manual transmission without a clutch between the motor and the transmission. To gearshift, the motor torque is first reduced to zero, then the first gear is disengaged, the motor is synchronized with the second gear, the second gear is engaged, and finally the motor driving torque is reapplied. Synchronizers may also help with the shaft synchronization and gear engagement [8, 9]. If properly performed, such a gearshift can have low jerk level, but a torque gap is inevitable, as the shifting elements have to be engaged and disengaged when no torque is passed through them. To reduce this torque gap, we can introduce a torque gap filler in the transmission architecture [10, 11]. This is typically a clutch placed between the motor and the transmission output shaft; it is used only during gearshift.

Alternatives to manual transmissions used in electric vehicles are dual clutch transmissions [12, 13, 14] and automatic transmissions [15, 16, 17, 18]. Conceptually, they are almost equivalent. Both consist of offering clutching and braking devices that can be modulated such that the transmission's torque can be continuously transferred between different transmission paths. The distinction resides in that dual clutch transmissions typically use a parallel shaft architecture and only require two clutches, while automatic transmissions typically use a planetary gearset architecture and require more clutching and braking devices if more than two gear ratios are to be offered. In both parallel shaft and planetary architectures, it can be interesting to replace a friction clutch by a one-way clutch [12, 16]. A one-way clutch that transfers the transmission torque in a given ratio will automatically disengage when a friction clutch of a higher gear ratio is engaged. This concept also allows to continuously transfer the torque between the two transmission paths, but with the added benefits that a one-way clutch is cheaper and more compact than a friction clutch or a brake.

Instead of using a multi-speed transmission, we could circumvent the drawbacks of having a single-motor fixed-ratio powertrain by using a plurality of motors. The different motors can be mounted on different axles, where the driving torque is shared through the road. Each motor can either power a single wheel [19] or a front or rear axle [20]. Alternatively, the different motors can also be mounted on the same axle [21]. These architectures allow the driving torque to be continuously transferred from one motor to another, thus providing excellent drivability. This is also true for multi-motor architectures with multi-speed transmissions. For instance, a planetary gearset architecture can be configured to receive inputs from two motors [22, 23, 24]. These transmission architectures are conceptually indistinguishable from power-split transmissions used in hybrid electric vehicles [25]. Alternatively, a parallel shaft architecture can be configured to receive inputs from two motors [26, 27]. Such a powertrain is capable of perfectly smooth gearshift: if the driving torque is taken exclusively from

one of the two motors, the other motor transmits no torque, which allows for an easy gear change on some transmission shafts. However, a torque gap may still exist, as the torque on one motor has to be reduced to zero and the other motor may not be able to fully compensate this torque decrease.

Finally, electric powertrains can also include mechanical continuously variable transmissions [28]. These powertrains provide excellent drivability, as the transmission ratio can be smoothly varied. However, there is a potential concern over a reduction in the powertrain energy efficiency [29].

From this review we conclude that concerns over drivetrain jerk are far greater when using a single-motor multi-speed transmission concept than any other powertrain concept. However, multi-speed transmissions remain good candidates for electric vehicle designers, as they may offer the best trade-off between conflicting requirements of cost, volume, weight, and energy efficiency for a given vehicle design. This motivates the focus of this study on gearshift jerk in single-motor multi-speed transmission powertrains.

1.2 Methodology

The existence of fundamental limitations to no-jerk gearshift that originate from motor saturation was hinted in [12], but such limitations were never formulated explicitly. In the literature, some studies on gearshift jerk reduction are framed around gearshift trajectory optimization [30, 31]. Typically, authors model a driveline, formulate a cost function that balances vehicle jerk and clutch energy dissipation, then solve a trajectory optimization problem. The main caveat with this approach is that often the optimization problem is non-convex, so a global optimum is not guaranteed. Moreover, it is hard to transfer the results to other vehicles or to slight alterations of the transmission. Other studies will address the design of an optimal gearshift controller instead [32, 33, 34, 35]. But similarly, we cannot easily generalize: we do not know if the vehicle jerk is a result of an imperfect controller, or a fundamental limitation we cannot avoid.

In this article, we take an inverse approach. After modelling the system, we first impose a jerk-free gearshift trajectory at the vehicle level. Then, we successively impose or compute trajectories for the remaining degrees of freedom, as well as the actuator signals – essentially a process of progressive variable elimination. When the only trajectories we find exceed the motor saturation limit, this means that a uninterrupted and jerk-free gearshift is impossible. We do not try to quantify the resulting level of jerk, as a proper assessment would require a complex and well calibrated vehicle model, [36] which also means that the conclusions would only be applicable to the specific vehicle studied. Instead, we focus on identifying the fundamental limitations that are true for any vehicle. Also in the interest of generality, we work under the assumption of perfect state feedback and a perfect control of actuator force. Formally, this translates into Assumption 1. Our results should therefore be interpreted as an upper bound on gearshift performance.

Assumption 1. Only the following two system limitations can lead to unavoidable gearshift jerk:

1. a limit on the motor torque, which can be characterized both in terms of maximal torque T_{\max} , or maximal power P_{\max} ;
2. a limit on the torque application rate of a friction clutch, dT/dt .

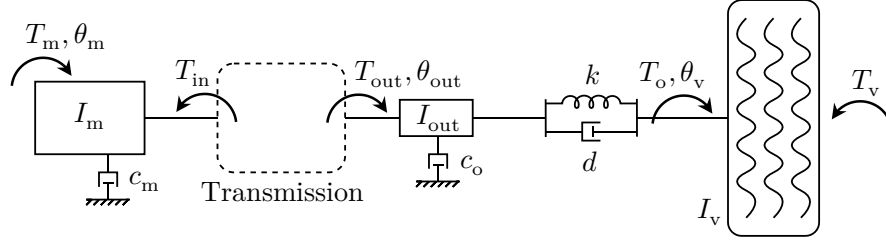


Figure 1: General driveline and vehicle model

In Section 2, we derive the equations of motion for vehicles equipped with the two transmissions presented in Figure 2, namely a two-speed dual-clutch transmission and a two-speed transmission based on planetary gearsets. In Section 3, we obtain realistic motor limitations through a motor selection process for an example vehicle, and illustrate the resulting gearshift trajectory limitations for selected shifting scenarios. Finally in Section 4, we present the theorems for the fundamental limitations to no-jerk gearshift resulting from actuator saturation.

2 Vehicle, driveline, and transmission modelling

In this section, we first present a generic vehicle and driveline model. We also introduce several transmission models, which are then embedded in the generic driveline model to compute the gearshift trajectories of Section 3.

2.1 Generic vehicle and driveline models

We begin with the generalized vehicle model. We assume that the vehicle longitudinal speed v follows the driving wheel speed $\dot{\theta}_v$ according to $v = \dot{\theta}_v r_w$, where r_w is the wheel radius. This allows to project the vehicle mass and the vehicular forces on the wheel coordinate. The vehicle mass m becomes an equivalent rotational inertia $I_v = m r_w^2$. In this model, we consider three vehicular forces: the aerodynamic drag F_{aero} , the tire rolling resistance F_{tire} , and gravity F_{slope} . These three forces become an equivalent torque T_v applied on the vehicle wheel as follows

$$T_v = r_w (F_{\text{aero}} + F_{\text{tire}} + F_{\text{slope}}) \quad (1)$$

$$T_v = r_w \left(\frac{1}{2} \rho A_f C_d v^2 + m g C_r \cos \alpha + m g \sin \alpha \right) \quad (2)$$

where ρ is the air density, A_f is the vehicle frontal area, C_d is the aerodynamic drag coefficient, C_r is the tire rolling resistance coefficient, g is gravity, and α is the road slope.

We use the driveline model shown on Figure 1. We have three rotating bodies: the electric motor I_m , the transmission output shaft I_{out} , and the equivalent vehicle inertia I_v . The three equations of motion for the general driveline and vehicle model are

$$I_m \ddot{\theta}_m = -c_m \dot{\theta}_m + T_m - T_{\text{in}} \quad (3)$$

$$I_{\text{out}} \ddot{\theta}_{\text{out}} = -c_o \dot{\theta}_{\text{out}} + T_{\text{out}} - k(\theta_{\text{out}} - \theta_v) - d(\dot{\theta}_{\text{out}} - \dot{\theta}_v) \quad (4)$$

$$I_v \ddot{\theta}_v = -T_v + k(\theta_{\text{out}} - \theta_v) + d(\dot{\theta}_{\text{out}} - \dot{\theta}_v) \quad (5)$$

where c_m is the coefficient of viscous damping on the motor, and c_o is the coefficient of viscous damping on the transmission output. The coefficients k and d represent lumped driveline stiffness and damping, respectively. They cover various phenomena such as driveshaft and driving tire flexibility and damping.

In this article, we are interested in finding gearshift trajectories that avoid vehicle jerk. Thus, we impose the kinematic constraint that $\ddot{\theta}_v = a_r/r_w$, where a_r is a prescribed and constant vehicle acceleration. By extension, we have that $\dot{\theta}_v = (a_r t + v_i)/r_w$, where v_i is the initial vehicle speed at the beginning of the gearshift ($t = 0$). Moreover, the trajectories we study only take place for a short amount of time – approximately 0.5 s – so it is fair to assume the vehicular forces T_v are constant. This allows us to group the vehicular forces and acceleration into a single constant output torque $T_o = I_v \ddot{\theta}_v + T_v$. Using Equation 5, we realize that $T_o = k(\theta_{out} - \theta_v) + d(\dot{\theta}_{out} - \dot{\theta}_v)$, which we can also use to simplify Equation 4. However, from Equation 5 we see that θ_{out} and $\dot{\theta}_{out}$ are also prescribed as a result of the no-jerk condition. Substituting $\ddot{\theta}_v$ and $\dot{\theta}_v$ with their no-jerk constraint, and taking the time derivative of Equation 5, we obtain a linear differential equation.

$$\ddot{\theta}_{out}(t) + \frac{k}{d}\dot{\theta}_{out}(t) = \frac{k}{dr_w}(a_r t + v_i) + \frac{a_r}{r_w} \quad (6)$$

We can solve this equation using the initial condition that $\dot{\theta}_{out}(0) = v_i/r_w$, and we get

$$\dot{\theta}_{out}(t) = \frac{a_r t + v_i}{r_w} \quad (7)$$

We now use the prescribed trajectories on $\dot{\theta}_v$, $\dot{\theta}_{out}$, and T_o to define a no-jerk gearshift as follows

Definition 1. A no-jerk gearshift is obtained if, for the duration of the gearshift,

$$\dot{\theta}_{out} = \dot{\theta}_v = (a_r t + v_i)/r_w \quad (8)$$

$$T_o = I_v a_r / r_w + T_v \quad (9)$$

Finally, the general vehicle and driveline model can be reduced to only two equations of motion as follows

$$I_m \ddot{\theta}_m = -c_m \dot{\theta}_m + T_m - T_{in} \quad (10)$$

$$I_{out} \ddot{\theta}_{out} = -c_o \dot{\theta}_{out} + T_{out} - T_o \quad (11)$$

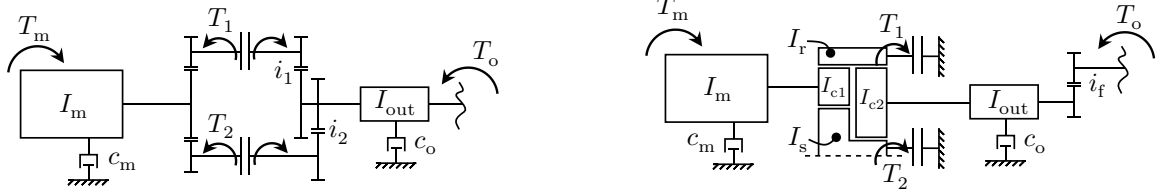
In the next sections, we transform the general model of Equations 10 and 11 into specific systems that depend on the transmission used, thereby replacing T_{in} and T_{out} by the relevant clutch, brake, and inertial torques.

2.2 Parallel shaft architecture with two frictional clutches

The first system model we build is that of the architecture illustrated in Figure 2a, when both clutches are frictional clutches. The equations of motion for this system are

$$I_m \ddot{\theta}_m = -c_m \dot{\theta}_m + T_m - T_1 - T_2 \quad (12)$$

$$I_{out} \ddot{\theta}_{out} = -c_o \dot{\theta}_{out} - T_o + i_1 T_1 + i_2 T_2 \quad (13)$$



(a) Two-speed transmission with parallel shaft architecture. Short name: dual-clutch transmission.

(b) Two-speed transmission with a planetary gearset architecture. Short name: dual-brake transmission.

Figure 2: The two powertrain architectures studied in this article.

where the clutch torques T_1 and T_2 depends on the state of the clutch – i.e. stick or slip. We assume a Coulomb friction model and we obtain the clutch torques as follows

$$T_1 = \begin{cases} T_m - T_2 - I_m \ddot{\theta}_m - c_m \dot{\theta}_m & \dot{\theta}_m = i_1 \dot{\theta}_{out} \\ F_{n1} \mu_d R_a n \text{sign}(\dot{\theta}_m - i_1 \dot{\theta}_{out}) & \dot{\theta}_m \neq i_1 \dot{\theta}_{out} \end{cases} \quad (14)$$

$$T_2 = \begin{cases} T_m - T_1 - I_m \ddot{\theta}_m - c_m \dot{\theta}_m & \dot{\theta}_m = i_2 \dot{\theta}_{out} \\ F_{n2} \mu_d R_a n \text{sign}(\dot{\theta}_m - i_2 \dot{\theta}_{out}) & \dot{\theta}_m \neq i_2 \dot{\theta}_{out} \end{cases} \quad (15)$$

where F_n is the linear force at the clutch plates, μ_d is the clutch's dynamic friction coefficient, R_a is the mean friction radius, and n is the number of friction surfaces. The clutch starts to slip when the reaction torque at the interface reaches the clutch torque capacity $T_{cap} = F_n \mu_s R_a n$, where μ_s is the static friction coefficient.

2.3 Parallel shaft architecture with a one-way clutch

For the system in Figure 2a, if we replace the first gear clutch by a one-way clutch, we have the same equations of motion, namely Equations 12 and 13. But T_1 is a reaction torque in one direction, and it is null in the other direction.

$$T_1 = \begin{cases} T_m - T_2 - I_m \ddot{\theta}_m - c_m \dot{\theta}_m & \dot{\theta}_m = i_1 \dot{\theta}_{out} \\ 0 & \dot{\theta}_m < i_1 \dot{\theta}_{out} \end{cases} \quad (16)$$

We also introduce a kinematic constraint such that $\dot{\theta}_m \leq i_1 \dot{\theta}_{out}$.

2.4 Planetary gearset architecture

In general, planetary gearsets have more degrees of freedom than parallel shaft architectures, thus they have more equations of motion. A single planetary stage can be seen as a combination of three bodies: a ring gear with inertia I_r , a planet carrier (I_c), and a sun gear (I_s). The equations of motion for each of these bodies in a single stage are

$$I_r \ddot{\theta}_r = T_r - N_r F \quad (17)$$

$$I_c \ddot{\theta}_c = T_c + N_r F + N_s F \quad (18)$$

$$I_s \ddot{\theta}_s = T_s - N_s F \quad (19)$$

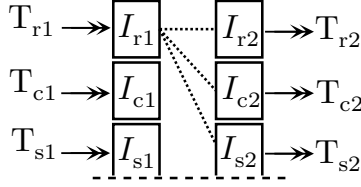


Figure 3: General representation of a double planetary gearset, where we show possible connections between the ring of the first set and elements of the second set. To operate as a transmission, a double planetary gearset must have three connections in total, which we obtain either by connecting elements together, or by grounding elements to the transmission casing. To change the transmission ratio, we simply change one of these connections.

where T_{\square} is the torque applied on either the ring (r), carrier (c), or sun (s), N_r is the number of teeth on the ring gear, N_s is the number of teeth on the sun gear, and F is the tooth force in the gearset. There is also a kinematic constraint associated with these equations

$$N_s \dot{\theta}_s + N_r \dot{\theta}_r = (N_s + N_r) \dot{\theta}_c \quad (20)$$

It is also common to combine planetary gearsets in series, such as in Figure 3. In this case, another set of three equations of motion are added to the system (Equations 17 to 19), as well as another kinematic constraint (Equation 20). By connecting elements, we reduce the number of degree of freedom in the system. These connections must be done carefully, as the system can become over-constrained or under-constrained. Transmission designers typically study numerous possible configurations before choosing the most suitable ones – a process named transmission synthesis [37], for which various methods exist ranging from using the classic lever analogy [38], to bond graphs [39]. A Ravigneaux planetary gearset can be seen as a special case of a double planetary gearset with its specific set of equations.

We are now ready to build the equations for the system in Figure 2b, which consists of a specific instance of a double planetary gearset architecture. The inertias I_m and I_{c1} are lumped into a single mass; we do the same for I_{out} and I_{c2} . We obtain the following equations of motion

$$I_r \ddot{\theta}_r = T_1 - N_{r1} F_1 - N_{r2} F_2 \quad (21)$$

$$I_m \ddot{\theta}_m = -c_m \dot{\theta}_m + T_m + N_{r1} F_1 + N_{s1} F_1 \quad (22)$$

$$I_{out} \ddot{\theta}_{out} = -c_o \dot{\theta}_{out} - i_f^{-1} T_o + N_{r2} F_2 + N_{s2} F_2 \quad (23)$$

$$I_s \ddot{\theta}_s = T_2 - N_{s1} F_1 - N_{s2} F_2 \quad (24)$$

and the following kinematic constraints

$$N_{s1} \dot{\theta}_s + N_{r1} \dot{\theta}_r = (N_{s1} + N_{r1}) \dot{\theta}_m \quad (25)$$

$$N_{s2} \dot{\theta}_s + N_{r2} \dot{\theta}_r = (N_{s2} + N_{r2}) \dot{\theta}_{out} \quad (26)$$

Using Equations 25 and 26, we can reduce the four equations of motion (Equations 21 to 24) into a set of two equations of motion. In order to solve this algebraic problem, researchers have assumed that elements other than the input and output shafts have negligible inertias, which simplifies the reduction process [40]. For the system of Figure 2b, it would mean that $I_r = 0$ and $I_s = 0$. When

Table 1: Example vehicle parameters

Param.	Value	Param.	Value	Param.	Value
m	6500 kg	I_{out}	0.05 kg m ²	i_2	6
r_w	0.3 m	c_m	0.02 Nm s/rad	I_r	0.03 kg m ²
A_f	6 m ²	c_o	0.04 Nm s/rad	I_s	0.03 kg m ²
C_d	0.7	k	10 kNm /rad	β_1	2
C_r	0.007	d	75 Nm s/rad	β_2	4
I_m	0.3 kg m ²	i_1	12	i_f	7.2

we make these assumptions, and introduce parameters $\beta_1 = N_{r1}/N_{s1}$ and $\beta_2 = N_{r2}/N_{s2}$, we get a set of equations that is identical in form to that of a parallel shaft architecture, only with different coefficients. This can be observed by comparing the equations 27 and 28 to the equations 12 and 13.

$$I_m \ddot{\theta}_m = -c_m \dot{\theta}_m + T_m + \frac{1 + \beta_1}{\beta_1 - \beta_2} T_1 - \frac{\beta_2(1 + \beta_1)}{\beta_1 - \beta_2} T_2 \quad (27)$$

$$I_{\text{out}} \ddot{\theta}_{\text{out}} = -c_o \dot{\theta}_{\text{out}} - i_f^{-1} T_o + \frac{1 + \beta_2}{\beta_2 - \beta_1} T_1 - \frac{\beta_1(1 + \beta_2)}{\beta_2 - \beta_1} T_2 \quad (28)$$

On the other hand, if we do not assume $I_r = I_s = 0$, we get a different system of equations, more coupled this time. Here, the constant coefficients C_1 to C_8 are not detailed further since they are rather involved algebraic expressions that only pertain to the specific architecture of Figure 2b. The important thing to realize is that the motor acceleration is now coupled with the transmission output.

$$I_m \ddot{\theta}_m = C_1(-c_m \dot{\theta}_m + T_m) + C_2(-c_o \dot{\theta}_{\text{out}} - i_f^{-1} T_o) + C_3 T_1 + C_4 T_2 \quad (29)$$

$$I_{\text{out}} \ddot{\theta}_{\text{out}} = C_5(-c_m \dot{\theta}_m + T_m) + C_6(-c_o \dot{\theta}_{\text{out}} - i_f^{-1} T_o) + C_7 T_1 + C_8 T_2 \quad (30)$$

3 Gearshift trajectories for an example vehicle

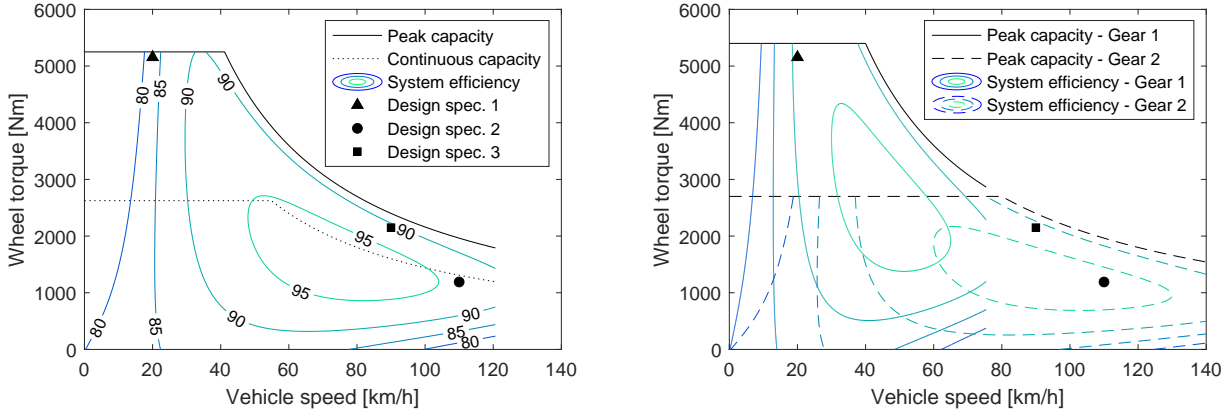
In Section 3.1, we obtain realistic motor limitations by mimicking a motor selection process for an example vehicle. Then in Section 3.2, using the transmission models obtained in Section 2, we illustrate the resulting limitations on gearshift dynamical trajectories. The example vehicle we hypothesize is a commercial vehicle for carrying goods. With a gross vehicle mass of 8500 kg, it would be classified as an N2 commercial vehicle in Europe, and a Class 5 medium-duty truck in North America. The vehicle and transmission parameters we use are shown in Table 1. Note that the gross vehicle mass of 8500 kg is used for the motor selection process, while the half-payload mass of 6500 kg presented in Table 1 is used for the gearshift trajectories.

3.1 Motor selection

We set the three design specifications of Table 2 to define the vehicle performance requirements. The first specification consists of an extreme grade; this sets the maximal torque requirement. This is a short duration event, so we allow the powertrain to be above its continuous capacity limit. The second specification consists of the vehicle cruising on a highway, which sets both a wheel speed requirement and a continuous power requirement. The third specification happens when the vehicle climbs a steep but reasonable grade on a highway, which sets the maximal power requirement.

Table 2: Design specifications considered in the motor selection

Design specification	v [km/h]	α [%]	Duration
1: extreme grade	20	20	< 1 min
2: highway, cruise speed	110	0	Continuous
3: highway, high grade	90	5	< 1 min



(a) Single speed transmission, ratio of 7.5. Motor requirements: 200 kW power, 700 Nm peak torque, and 8000 rpm maximum speed.

(b) Two-speed transmission, ratios of 12 and 6. Motor requirements: 200 kW power, 450 Nm peak torque, and 8000 rpm maximum speed.

Figure 4: Vehicle capacity for (a) a single speed transmission and (b) a two-speed transmission.

As shown in Figure 4a, if the vehicle is equipped with single speed transmission, the vehicle requirements can be met with a 200 kW motor with 700 Nm peak torque and 8000 rpm maximum speed, using a fixed total reduction ratio of 7.5. With a two-speed transmission with ratios of 12 and 6, we can lower the peak torque requirement to 450 Nm, while keeping the same power and speed limits. In practice, this could be achieved by scaling the motor’s active length [41]. We display the resulting system capacity in Figure 4b. The vehicle now has a 36 % smaller motor and a larger high-efficiency operating region.

3.2 Gearshift Trajectories

In this section, we present five example gearshift trajectories. More specifically, we study the three gearshift scenarios presented in Table 3. Scenario 1 is an upshift during vehicle acceleration, where the driver torque demand (DTD) at the beginning of the shift is 80 % of available torque. This gearshift takes place in the power-limited region of the motor map. Scenario 2 is a downshift when the vehicle is accelerating, also with a DTD of 80 %. The downshift takes place in the torque-limited

Table 3: Gearshift scenarios

Scenario	Direction	Motor quadrant	v_i [km/h]	a_r [m/s ²]	DTD
1	Upshift	Driving	65	1.0	80 %
2	Downshift	Driving	18	1.0	80 %
3	Downshift	Braking	45	-1.5	-

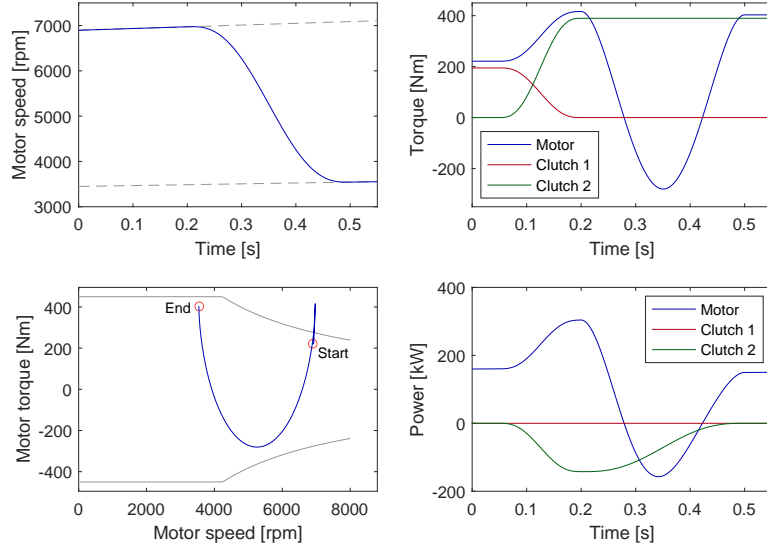


Figure 5: Example trajectory for the gearshift scenario 1 with a dual-clutch transmission, where the first clutch is a one-way clutch.

region of the motor map. This gearshift is justified by the desire to have a greater wheel torque after the downshift. Scenario 3 is a downshift when the motor is used for regenerative braking.

The trajectory of Figure 5 is an upshift during vehicle acceleration (scenario 1) for the case where the transmission is a parallel shaft architecture, and the first clutch is a one-way clutch. The gearshift starts at 0.05 s and ends at 0.50 s; it consists of a torque phase followed by an inertia phase. During the torque phase, we gradually increase T_2 , imposing an arbitrary trajectory from zero torque up to the torque level required when the transmission is in second gear. We also increase the motor torque T_m , so that the reaction torque T_1 is such that we maintain a constant output torque T_o , which is a condition for a no-jerk gearshift. From Equations 12 and 13, we notice that because $i_1 > i_2$, the torque phase inevitably results in an increase in the motor torque. Because the first clutch is a one-way clutch, this is the only possible trajectory for the system. Since the motor power exceeds the 200 kW limit, the trajectory is infeasible. In reality, we would inevitably experience a torque gap and a vehicle jerk. This consists of the first fundamental limitation we explore in this article, see Theorem 1 in the next section. The rest of the gearshift consists of the inertia phase, which is not as prone to motor saturation as the torque phase. We keep T_1 and T_2 constant, and we synchronize the motor with the gear 2 speed using an appropriate but arbitrary trajectory.

The trajectory of Figure 6 is also an upshift during vehicle acceleration, also for a parallel shaft architecture, but this time clutch 1 is a friction clutch. This introduces two new possibilities: we can increase the motor speed above the gear 1 speed, and we can modulate T_1 when the clutch is slipping. We take advantage of these possibilities and craft a new trajectory that results in a no-jerk gearshift. Prior to transferring the clutch torques, we increase the motor speed above the gear 1 speed, up to a prescribed value. We then begin the torque transfer, which has the effect of decreasing the motor speed. It is important that we complete the torque transfer before the motor crosses the gear 1 speed, as this would result in a sign reversal on T_1 . Recall that when a friction clutch slips,

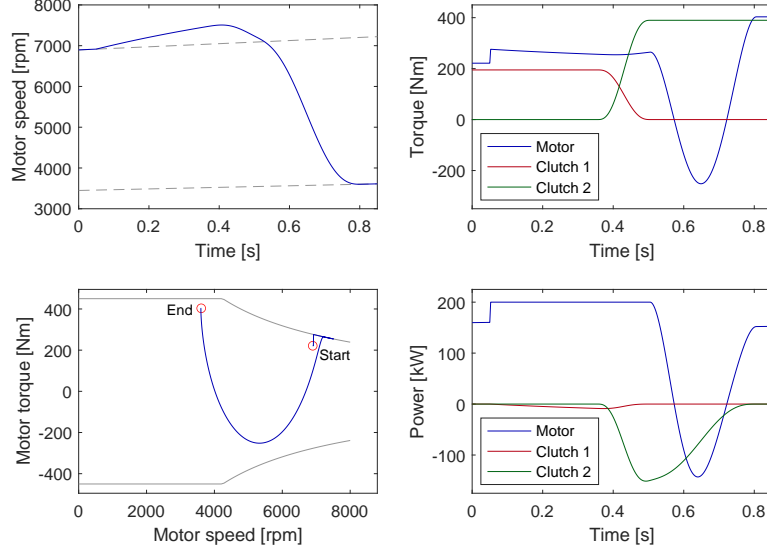


Figure 6: Example trajectory for the gearshift scenario 1 with a dual-clutch transmission, where the first clutch is a friction clutch.

the clutch torque opposes the clutch slipping velocity, see Equation 14 for instance. A torque reversal on T_1 would mean that T_2 has to instantaneously compensate in order to maintain the constant T_o condition. This is likely to violate any constraint on the clutch torque application rate. Therefore, this new trajectory also contains a fundamental limitation, which is formulated in Theorem 2.

The trajectory of Figure 7 is a downshift during motor acceleration (scenario 2), with a parallel shaft architecture. This trajectory can be obtainable for both the cases where the first clutch is a one-way clutch or a friction clutch. This time we proceed with the inertia phase before the torque phase. In the inertia phase, we increase the motor speed using maximal motor power. When the motor reaches gear 1 speed, the torque transfer begins. This time, the fundamental limitation consists of being able to synchronize the motor speed within an acceptable time while maintaining the output torque T_o constant. This limitation is formalized in Theorem 3.

The trajectory of Figure 8 is a downshift during vehicle deceleration (scenario 3). More specifically, the motor operates in regenerative braking mode. We have that $T_o < 0$, which also means that $T_m < 0$, $T_1 < 0$, and $T_2 < 0$. Because $T_1 < 0$, this trajectory is only possible if clutch 1 is a friction clutch. A one-way clutch can only carry torque in one direction – i.e. the positive direction in our case. Often, transmissions with a one-way clutch are also equipped with a locking mechanism in parallel to the one-way clutch [12]. This allows for regenerative braking when the transmission operates in first gear. However, this locking mechanism cannot be applied when there is a significant speed difference between the elements, and it cannot be modulated. Therefore, it is impossible for a dual-clutch transmission with a one-way clutch to provide uninterrupted shifting in regenerative braking mode. Figure 8 shows that for a dual friction clutch architecture, such a gearshift can be initiated even when the motor is essentially on the saturation limit.

In the trajectory of Figure 9, we come back to gearshift scenario 1, but with the dual-brake

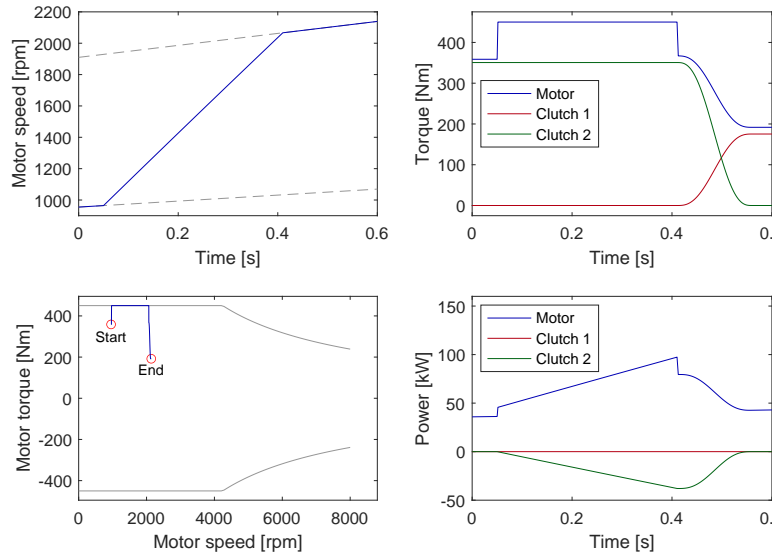


Figure 7: Example trajectory for the gearshift scenario 2 with a dual-clutch transmission. This trajectory is valid for both one-way clutch and dual-friction-clutch architectures.

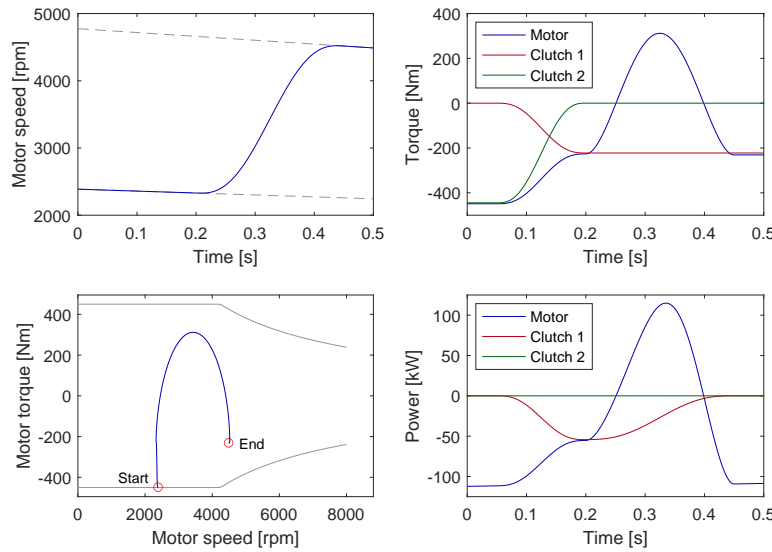


Figure 8: Example trajectory for the gearshift scenario 3 with a dual-clutch transmission. This trajectory is only possible if clutch 1 is of friction type.

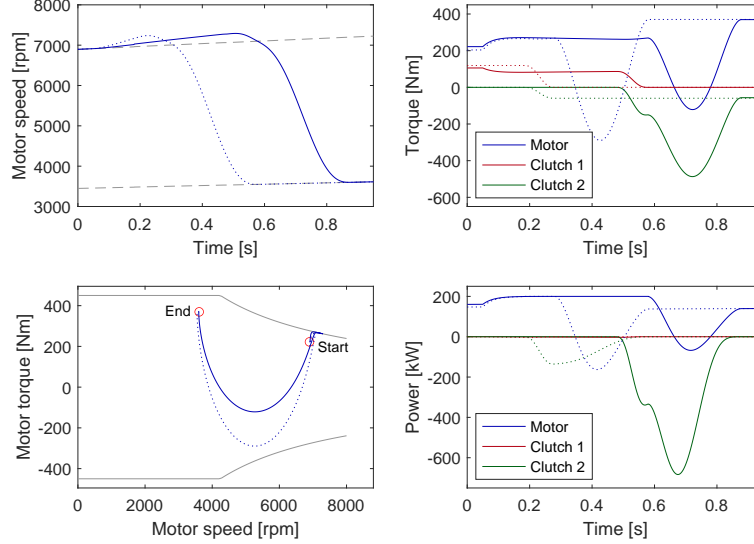


Figure 9: Example trajectories for the gearshift scenario 1 with a dual-brake transmission, namely that of Figure 2b. The dotted lines represent the situation where we set $I_r = I_s = 0$. The solid lines represent the situation where we include the inertia of I_r and I_s .

transmission of Figure 2b this time. In terms of trajectory, we follow the same strategy as that of Figure 6, i.e., increasing the motor speed above the gear 1 speed before proceeding with the torque transfer. If we assume $I_r = I_s = 0$, we obtain the trajectory in dotted lines. But if we have that $I_r = I_s = I_m/10$, we obtain the trajectory in solid lines. The introduction of a small inertia on I_r and I_s has a strong influence on the resulting trajectory. First, we notice that T_m becomes coupled with T_1 . In other words, when we increase the motor torque in the first phase of the gearshift, we have to decrease T_1 in order to maintain the same output torque T_o . This means we cannot increase T_m arbitrarily quickly; we have to respect the clutch torque application rate limitation. Also, we notice that the additional inertia increases the time required to attain a given motor speed during the first phase. Finally, clutch 2 takes a larger portion of the load during the inertia phase, and the motor takes a smaller portion of the load. From a design perspective, this means the maximal torque requirement on clutch 2 is higher, which has to be accounted for in the sizing of this component. In conclusion, even small inertia can have a significant influence on the gearshift trajectory of a transmission with a planetary gearset architecture. Engineers should take precaution before neglecting them in the equations of motion for their systems.

4 Fundamental limitations to no-jerk gearshift

In Section 4.1, we introduce three theorems that define the fundamental limitations to no-jerk gearshift for a dual-clutch transmission – they are summarized in Table 4. Then in Section 4.2, we adapt these theorems for transmissions based on planetary gearsets.

4.1 Theorems for fundamental limitations with a dual clutch architecture

In Theorem 1, we express a necessary and sufficient condition such that we can have no-jerk upshift in the power-limited region of the motor, when clutch 1 is a one-way clutch. We can use Equation 31

Table 4: Summary of fundamental gearshift limitations for the dual-clutch transmission

Scenario	One-Way Clutch	Dual Friction Clutch
1: Upshift, driving motor	Limited by Theorem 1	Limited by Theorem 2
2: Downshift, driving motor	Limited by Theorem 3	Limited by Theorem 3
3: Downshift, braking motor	Impossible	Not limited

and the assumptions that $\dot{\theta}_{\text{out}}(t) = (a_{\text{r}}t + v_{\text{i}})/r_{\text{w}}$ and $\ddot{\theta}_{\text{out}}(t) = a_{\text{r}}/r_{\text{w}}$ to predict if a specific driving condition allows for a no-jerk gearshift; we do not need to simulate the gearshift.

Theorem 1. *For a dual clutch architecture were the first gear clutch is a one-way clutch, when the motor operates in a power-limited region, a no-jerk upshift of scenario 1 can be obtained if and only if $P_{\text{m}}(t_{\text{tr}}) \leq P_{\text{max}}$, where $P_{\text{m}}(t_{\text{tr}})$ is the required motor power at the end of the torque transfer phase, and P_{max} is the motor power limit; $P_{\text{m}}(t_{\text{tr}})$ can be evaluated as*

$$P_{\text{m}}(t_{\text{tr}}) = i_1 \dot{\theta}_{\text{out}}(t_{\text{tr}}) \left((i_1 I_{\text{m}} + i_2^{-1} I_{\text{out}}) \ddot{\theta}_{\text{out}}(t_{\text{tr}}) + (i_1 c_{\text{m}} + i_2^{-1} c_{\text{o}}) \dot{\theta}_{\text{out}}(t_{\text{tr}}) + i_2^{-1} T_{\text{o}} \right) \quad (31)$$

Proof. (Necessity): The gearshift begins with a torque transfer phase that spans from $t = 0$ to $t = t_{\text{tr}}$, which is defined as follows: the clutch torques are smoothly varied from $T_1(0) \neq 0$ and $T_2(0) = 0$ to $T_1(t_{\text{tr}}) = 0$ and $T_2(t_{\text{tr}}) \neq 0$, while $\dot{\theta}_{\text{m}} = i_1 \dot{\theta}_{\text{out}}$ and $\ddot{\theta}_{\text{m}} = i_1 \ddot{\theta}_{\text{out}}$ for all $t \in [0, t_{\text{tr}}]$, and T_{o} , $\dot{\theta}_{\text{out}}$, and $\ddot{\theta}_{\text{out}}$ follow the conditions for a no-jerk gearshift as per Definition 1. The condition $\dot{\theta}_{\text{m}} = i_1 \dot{\theta}_{\text{out}}$ is necessary because the first gear clutch is a one-way clutch: Equation 16 indicates that $T_1 \neq 0 \rightarrow \dot{\theta}_{\text{m}} = i_1 \dot{\theta}_{\text{out}}$, so this imposes $\dot{\theta}_{\text{m}} = i_1 \dot{\theta}_{\text{out}}$ at least until $T_1 = 0$. The condition $\ddot{\theta}_{\text{m}} = i_1 \ddot{\theta}_{\text{out}}$ is necessary for a no-jerk gearshift: Equation 16 indicates that if the clutch opens before $T_1 = 0$, which means we would have $\dot{\theta}_{\text{m}} < i_1 \dot{\theta}_{\text{out}}$, then the clutch torque immediately drops to 0, and Equation 13 indicates that for T_{o} , $\dot{\theta}_{\text{out}}$, and $\ddot{\theta}_{\text{out}}$ to follow the conditions for a no-jerk gearshift, then T_2 would have to immediately jump to a higher value, which violates the limit on clutch torque application rate. Moreover, the one-way clutch imposes the kinematic constraint that $\dot{\theta}_{\text{m}} \leq i_1 \dot{\theta}_{\text{out}}$, so if we have that $\dot{\theta}_{\text{m}} = i_1 \dot{\theta}_{\text{out}}$, we cannot have that $\dot{\theta}_{\text{m}} > i_1 \dot{\theta}_{\text{out}}$. Thus, we showed that the torque transfer phase as defined above is necessary for a no-jerk gearshift, as any deviation from it either implies a vehicle jerk, or is physically impossible. We now find the required motor power at the end of the torque phase. With $T_1(t_{\text{tr}}) = 0$ in Equation 13, we get that

$$T_2(t_{\text{tr}}) = i_2^{-1} \left(I_{\text{out}} \ddot{\theta}_{\text{out}}(t_{\text{tr}}) + c_{\text{o}} \dot{\theta}_{\text{out}}(t_{\text{tr}}) + T_{\text{o}} \right) \quad (32)$$

which we can substitute in Equation 12 to get the motor torque at t_{tr}

$$T_{\text{m}}(t_{\text{tr}}) = I_{\text{m}} \ddot{\theta}_{\text{m}}(t_{\text{tr}}) + c_{\text{m}} \dot{\theta}_{\text{m}}(t_{\text{tr}}) + i_2^{-1} \left(I_{\text{out}} \ddot{\theta}_{\text{out}}(t_{\text{tr}}) + c_{\text{o}} \dot{\theta}_{\text{out}}(t_{\text{tr}}) + T_{\text{o}} \right) \quad (33)$$

We find the required motor power at t_{tr} using $P_{\text{m}}(t_{\text{tr}}) = \dot{\theta}_{\text{m}}(t_{\text{tr}}) T_{\text{m}}(t_{\text{tr}})$, Equation 33, and the conditions that $\dot{\theta}_{\text{m}}(t_{\text{tr}}) = i_1 \dot{\theta}_{\text{out}}(t_{\text{tr}})$ and $\ddot{\theta}_{\text{m}}(t_{\text{tr}}) = i_1 \ddot{\theta}_{\text{out}}(t_{\text{tr}})$; we obtain Equation 31. We now have that a no-jerk gearshift requires a motor power $P_{\text{m}}(t_{\text{tr}})$ as described in (31). Naturally, this requires that the motor is capable of producing $P_{\text{m}}(t_{\text{tr}})$, so we have that a no-jerk gearshift implies that $P_{\text{m}}(t_{\text{tr}}) \leq P_{\text{max}}$.

(Sufficiency): Assumption 1 indicates that if we cannot obtain a no-jerk gearshift, it is because either the motor saturates, or the clutch saturates. Further assuming we can always have t_{tr} large enough such that the clutch application rate does not saturate, we have that if we cannot obtain a

no-jerk gearshift, it is because the motor saturates. By showing that $P_m(t_{\text{tr}})$ is the maximal required motor power during the gearshift, we can show that if the motor saturates, we must have that $P_m(t_{\text{tr}}) > P_{\text{max}}$. We rearrange Equations 12 and 13 to eliminate T_2 and isolate T_m , and we get the motor power as follows

$$P_m = \dot{\theta}_m \left(I_m \ddot{\theta}_m + c_m \dot{\theta}_m + T_1 \left(1 - \frac{i_1}{i_2} \right) + i_2^{-1} \left(I_{\text{out}} \ddot{\theta}_{\text{out}} + c_o \dot{\theta}_{\text{out}} + T_o \right) \right) \quad (34)$$

Assuming that we begin to synchronize the motor with the second gear speed the instant the torque transfer is complete at t_{tr} , we have that the maximal $\dot{\theta}_m(t)$ is at $t = t_{\text{tr}}$. We now have that every term on the right hand side of Equation 34 is maximized at t_{tr} . In particular, we notice that since $i_1 > i_2$, we have that $T_1(t_{\text{tr}}) = 0$ maximizes P_m , as $T_1 \geq 0$. Therefore, if we cannot obtain a no-jerk gearshift, then $P_m(t_{\text{tr}}) > P_{\text{max}}$. \square

In Theorem 2, we express a necessary and sufficient condition such that we can have a no-jerk upshift (gearshift scenario 1) in the power-limited region of the motor, when clutch 1 is a friction clutch. We follow the strategy detailed in Figure 10. To give the reader a visual appreciation of the limitations, we also simulated several instances of this strategy, which we display in Figure 11. In practice, we can use Theorem 2 to predict if a specific driving condition allows us to proceed with a no-jerk gearshift. Because Equation 38 makes it such that the equations of motion for the system become nonlinear, there may not be a convenient closed form solution to facilitate the process of finding a sufficient Δ_m . Perhaps the best way to do so is to simulate the first phase of the gearshift up to a given Δ_m , and then validate if this Δ_m is sufficient to allow a complete torque transfer before $\Delta_s = 0$. If the given Δ_m is not sufficient, then the process can be repeated for a higher Δ_m , until no higher Δ_m can be reached, at which point we can conclude a no-jerk trajectory is infeasible.

Theorem 2. *Consider a dual clutch architecture with two friction clutches as shown in Figure 2a. Referring to Figure 10, suppose that at $t = 0$ the motor speed is synchronized with gear 1's speed and that it is desired to initiate a gearshift to be completed at time t_2 . Let $t_{\text{tr}} > 0$ be the set torque transfer duration in the gearshift and t_1 the time at which the torque transfer is initiated. When the motor operates in a power-limited region, a no-jerk upshift of scenario 1 can be obtained if and only if*

$$\exists \Delta_m := \dot{\theta}_m(t_1) - i_1 \dot{\theta}_{\text{out}}(t_1) \geq 0, \quad (35)$$

$$\text{s.t. } \Delta_s := \dot{\theta}_m(t_1 + t_{\text{tr}}) - i_1 \dot{\theta}_{\text{out}}(t_1 + t_{\text{tr}}) \geq 0, \quad (36)$$

$$\dot{\theta}_m(t_1) \leq \dot{\theta}_{\text{max}}, \quad (37)$$

$$\text{where } T_m(t) = P_{\text{max}}/\dot{\theta}_m(t), \quad 0 \leq t \leq t_1 + t_{\text{tr}} \quad (38)$$

$$T_1(t) = 0, \quad t_1 + t_{\text{tr}} \leq t \leq t_2 \quad (39)$$

$$T_2(t) = 0, \quad 0 \leq t \leq t_1 \quad (40)$$

Proof. (Necessity): The gearshift begins with a speed phase ($0 \leq t \leq t_1$), where the motor speed is increased above $i_1 \dot{\theta}_{\text{out}}$, with $T_2 = 0$ and $T_m = P_{\text{max}}/\dot{\theta}_m$. Then the gearshift continues with a torque transfer phase ($t_1 \leq t \leq t_1 + t_{\text{tr}}$), where the clutch torques are smoothly varied from $T_1(t_1) \neq 0$ and $T_2(t_1) = 0$ to $T_1(t_1 + t_{\text{tr}}) = 0$ and $T_2(t_1 + t_{\text{tr}}) \neq 0$, while $T_m = P_{\text{max}}/\dot{\theta}_m$. Finally, the gearshift ends with an inertia phase ($t_1 + t_{\text{tr}} \leq t \leq t_2$), where the motor speed is brought down to $i_2 \dot{\theta}_{\text{out}}$, while $T_1 = 0$. During all three phases, the conditions for a no-jerk gearshift in Definition 1 can be maintained by modulating T_1 and T_2 as per Equation 13. Motor saturation can be avoided as the motor torque is set to $T_m = P_{\text{max}}/\dot{\theta}_m$ for the first two phases, and the motor synchronization of

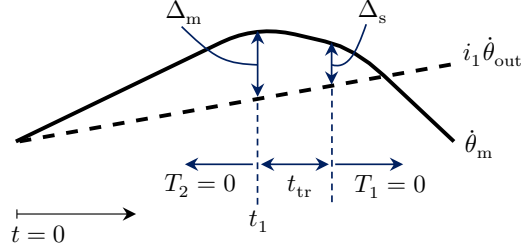


Figure 10: Strategy for a power-on upshift with a dual-friction clutch transmission. We first increase the motor speed to an increment Δ_m above the gear 1 speed. Once Δ_m is reached, we begin the torque transfer, which takes a set time t_{tr} . At the end of the torque transfer, the motor will have decelerated to a different speed whose increment over gear 1 speed which we define as Δ_s . In order to avoid torque reversal at clutch 1, which would imply an unavoidable jerk, we must have that $\Delta_s \geq 0$.

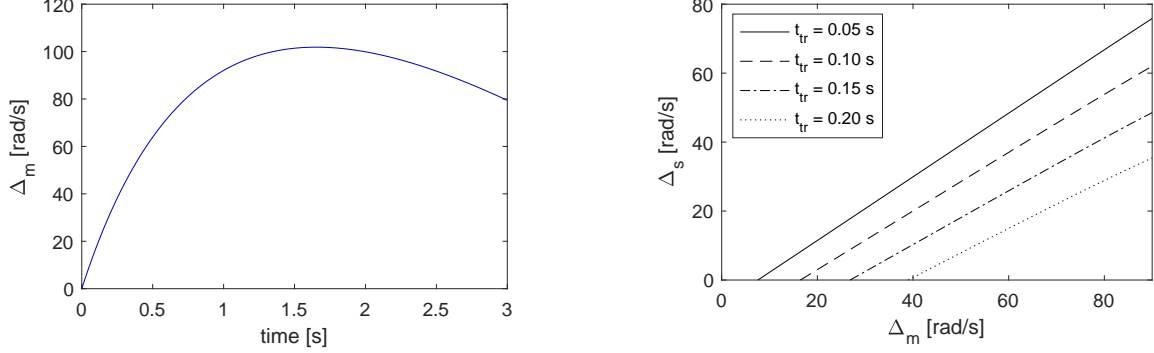
the inertia phase requires that $T_m < P_{max}/\dot{\theta}_m$. The torque application rate on both clutches can be maintained within limits during the speed phase, as $T_2 = 0$ and the variations on T_o , $\dot{\theta}_{out}$, and $\ddot{\theta}_{out}$ are small enough such that dT_1/dt is within limits. The same argument can be made for the inertia phase, with $T_1 = 0$ this time. During the torque transfer phase, appropriate clutch torque trajectories must be chosen such that limits on dT/dt are respected. Moreover, a torque reversal on clutch 1 must be avoided.

In effect, the clutch torque T_1 is necessarily positive when the motor is driving the vehicle through the first gear and clutch 1 sticks. When clutch 1 slips, the direction of T_1 is dependent on the slip direction, as described in Equation 14. If $\dot{\theta}_m < i_1 \dot{\theta}_{out}$, then the torque T_1 suddenly reverses direction and becomes negative. In order to maintain the conditions for a no-jerk gearshift, Equation 13 indicates that the torque reversal on T_1 must be instantaneously compensated by an increase in T_2 , which necessarily violates any application rate limitation. Consequently, we must have that $\dot{\theta}_m \geq i_1 \dot{\theta}_{out}$ as long as $T_1 \neq 0$. Once we begin the torque transfer phase, we have that $\ddot{\theta}_m(t) < \ddot{\theta}_m(t_1)$, as $i_1 > i_2$, which can be seen from Equations 12 and 13. Therefore, we need to start the torque transfer at a sufficiently high Δ_m such that $\Delta_s \geq 0$. Moreover, we must have that Δ_m is such that the motor speed is within the motor speed limit $\dot{\theta}_{max}$. However, nothing guarantees the system can reach such a Δ_m . If we fail to reach a satisfactory Δ_m , then one of the conditions for a no-jerk gearshift will not be respected due to system limitations – there will be jerk. This proves the necessity part by contraposition.

(Sufficiency): By construction, the actuation strategy described in Equations 38 to 40 is sufficient for a no-jerk gearshift, given that Assumption 1 holds.

This actuation strategy is not unique, but any deviation would only make it harder to achieve a sufficiently high Δ_m . Consequently, if a no-jerk gearshift can be obtained using such a deviation from Equations 38 to 40, it can also be obtained using the actuation strategy described in these equations. Therefore, if we cannot obtain a no-jerk gearshift, we cannot find a Δ_m such that $\Delta_s \geq 0$ following Equations 38 to 40. \square

In Theorem 3, we express a necessary and sufficient condition such that we can have a no-jerk downshift (gearshift scenario 2) in the torque limited region of the motor. This limitation is the same for both when the first clutch is a one-way clutch or a friction clutch. The limitation is illustrated in Figure 12. We simulated several instances of gearshift scenarios 2, where we varied the initial vehicle acceleration a_r . We recorded the required time for the motor to synchronize with the first gear speed,



(a) Even when using the maximum available motor power, not all Δ_m can be reached.

(b) The resulting Δ_s after the torque transfer is a function of the starting Δ_m and the transfer time t_{tr} .

Figure 11: Example of limitations for a power-on upshift with the example vehicle and a dual-friction-clutch transmission, when the gearshift is initiated at $v_i = 65$ km/h, and $a_r = 1.0$ m/s²

which we label t_s . When a_r is too high, either t_s is impractically long, or the motor never synchronizes with the first gear speed.

Theorem 3. *For a dual clutch architecture with two friction clutches, when the motor operates in a torque-limited region, a no-jerk power-on downshift of scenario 2 can be obtained if and only if*

$$\exists t_s > 0 \quad \text{s.t.} \quad 0 = -i_1 \frac{v_i + a_r t_s}{r_w} + \exp\left(-\frac{c_m}{I_m} t_s\right) i_2 \frac{v_i}{r_w} + \frac{T_{\max} - T_2}{c_m} \left[1 - \exp\left(-\frac{c_m}{I_m} t_s\right)\right] \quad (41)$$

Proof. (Necessity): The gearshift begins with an inertia phase ($0 \leq t \leq t_s$), where $\dot{\theta}_m$ is accelerated from gear 2 synchronization speed to gear 1 synchronization speed, while $T_m = T_{\max}$ and $T_1 = 0$. The gearshift ends with a torque phase ($t_s \leq t \leq t_s + t_{tr}$), where the transmission torque is transferred from clutch 2 to clutch 1. During both phases, the conditions for a no-jerk gearshift in Definition 1 can be maintained by modulating T_1 and T_2 as per Equation 13. Motor saturation can be avoided by restricting the motor power to $T_m \leq T_{\max}$. Clutch torque application rate saturation can be avoided by using an appropriate torque transfer trajectory during the torque phase. However, when using these restrictions together, nothing guarantees that the motor will eventually synchronize with gear 1 speed at some time t_s . We now find an equation that describes the synchronization time t_s when the no-jerk gearshift conditions are maintained. With $T_m = T_{\max}$ and $T_1 = 0$ in Equation 12, we get the motor acceleration

$$\ddot{\theta}_m = I_m^{-1} \left(-c_m \dot{\theta}_m + T_{\max} - T_2\right) \quad (42)$$

We assume T_2 is constant during the inertia phase. This makes Equation 42 a linear ordinary differential equation, which we solve to get the evolution of $\dot{\theta}_m(t)$. We impose the initial condition that $\dot{\theta}_m(0) = i_2 \dot{\theta}_{\text{out}}(0)$, and we get

$$\dot{\theta}_m(t) = \exp\left(-\frac{c_m}{I_m} t\right) i_2 \dot{\theta}_{\text{out}}(0) + \frac{T_{\max} - T_2}{c_m} \left[1 - \exp\left(-\frac{c_m}{I_m} t\right)\right] \quad (43)$$

When the motor synchronizes with the gear 1 speed, we have that $\dot{\theta}_m = i_1 \dot{\theta}_{\text{out}}$. Substituting this condition into Equation 43, and using the fact that $\dot{\theta}_{\text{out}}(t) = (v_i + a_r t)/r_w$, we obtain Equation 41. For the motor to synchronize with gear 1 speed, Equation 41 must have a solution. Therefore, if

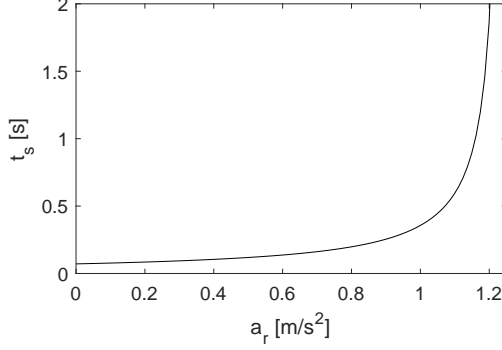


Figure 12: Example of limitations for a power-on downshift with the example vehicle, when the gearshift is initiated at $v_i = 18\text{ km/h}$, and a_r is varied. When the desired vehicle acceleration a_r is increased, the time t_s required for the inertia phase to complete also increases.

Equation 41 has no solution for t_s , then a no-jerk gearshift cannot be obtained, which proves the necessity part by contraposition.

(Sufficiency): By construction, the actuation strategy described in the first paragraph of this proof is sufficient for a no-jerk gearshift, given that Assumption 1 holds.

This actuation strategy is not unique. We could have $T_m < T_{\max}$, but it would only make it harder to synchronize the motor with gear 1 speed, which can be seen from Equation 42. If clutch 1 is a one-way clutch, then we must have $T_1 = 0$ until the motor synchronizes with gear 1 speed, as per Equation 16. If clutch 1 is a friction clutch, then it is possible to activate T_1 before t_s . But from Equation 14, we notice that we would have $T_1 < 0$, so Equation 13 dictates that T_2 increases by $|T_1|(i_1/i_2)$ to respect the no-jerk conditions, and since $i_1 > i_2$, $\ddot{\theta}_m$ would again be smaller than if $T_1 = 0$. Therefore, if a no-jerk gearshift can be completed with a different actuation strategy than the one presented in the necessity part of the proof, it can also be completed with this strategy. As a result, the existence of a solution to Equation 41 is a sufficient condition for the possibility of a no-jerk gearshift. \square

4.2 Theorem adaptations for planetary gearset architectures

In this section, we adapt Theorems 1 to 3 to planetary gearset architectures described by the general Equations 29 and 30.

4.2.1 Theorem 1

With the new system equations, the motor power at the end of the torque transfer phase – originally described by Equation 31 – now becomes

$$P_m(t_{\text{tr}}) = i_1 \dot{\theta}_{\text{out}}(t_{\text{tr}}) \left(c_m i_1 \dot{\theta}_{\text{out}}(t_{\text{tr}}) + \left(C_1 - \frac{C_4 C_5}{C_8} \right)^{-1} \left[\left(i_1 I_m - \frac{C_4}{C_8} I_{\text{out}} \right) \ddot{\theta}_{\text{out}}(t_{\text{tr}}) + \left(C_2 - \frac{C_4 C_6}{C_8} \right) (c_o \dot{\theta}_{\text{out}}(t_{\text{tr}}) + i_f^{-1} T_o) \right] \right) \quad (44)$$

The proof for the necessity condition remains valid, as it is based on the limitations imposed by the one-way clutch, and these limitations still apply. The proof for the sufficiency condition requires to demonstrate that $P_m(t_{tr})$ is the maximal motor power required during the gearshift, which now ultimately depends on the coefficients C_1 to C_8 , as can be seen by adapting Equation 34 into a new expression for the motor power

$$P_m = \dot{\theta}_m \left(c_m \dot{\theta}_m + \left(C_1 - \frac{C_4 C_5}{C_8} \right)^{-1} \left[I_m \ddot{\theta}_m - \frac{C_4}{C_8} I_{out} \ddot{\theta}_{out} + \left(C_2 - \frac{C_4 C_6}{C_8} \right) (c_o \dot{\theta}_{out} + i_f^{-1} T_o) - \left(C_3 - \frac{C_4 C_7}{C_8} \right) T_1 \right] \right) \quad (45)$$

In particular, for $T_1 = 0$ to maximize P_m , we must have that $-(C_3 - C_4 C_7 / C_8)(C_1 - C_4 C_5 / C_8)^{-1} < 0$. For the architecture in Figure 2b, this expression reduces to $-(\beta_1 + 1) / \beta_1$, so we have that indeed $T_1 = 0$ maximizes P_m since $-(\beta_1 + 1) / \beta_1 < 0$. Assuming that the other variables – i.e. $\dot{\theta}_m$, $\ddot{\theta}_m$, $\dot{\theta}_{out}$, $\ddot{\theta}_{out}$, and T_o – remain approximately constant during the torque phase, we have that $P_m(t_{tr})$ is the maximal motor power required during the gearshift for the case of the architecture in Figure 2b.

4.2.2 Theorem 2

The existence of a sufficient Δ_m such that $\Delta_s \geq 0$ remains a necessary and sufficient condition for the possibility of a no-jerk gearshift. The only difference is that we cannot have T_m jumping to $P_{max} / \dot{\theta}_m$ at $t = 0$, as prescribed in Equation 38. In effect, T_m now appears in the second equation of motion of the system, i.e. Equation 30, so if we wish to maintain T_o , $\dot{\theta}_m$, and $\ddot{\theta}_m$ such that the no-jerk conditions in Definition 1 are met, a sudden increase in T_m implies a sudden increase in T_1 (as we impose $T_2(0) = 0$), which necessarily violates any torque application rate limitation. The effect of an increase in T_m on T_1 can be seen in Figure 9. So Theorem 2 remains valid, but we must ramp up T_m such that dT/dt is within limits.

4.2.3 Theorem 3

The proof for Theorem 3 remains valid, but the necessary and sufficient condition described by Equation 41 must be adapted to the new system equations. First, we get $\dot{\theta}_m$ during the inertia phase by imposing $T_1 = 0$ in Equations 29 and 30; we get

$$\ddot{\theta}_m = I_m^{-1} \left(-\gamma c_m \dot{\theta}_m + \gamma T_m - \tau \right) \quad (46)$$

$$\gamma = \left(C_1 - \frac{C_4 C_5}{C_8} \right) \quad (47)$$

$$\tau = \left(C_2 - \frac{C_4 C_6}{C_8} \right) (c_o \dot{\theta}_{out} + i_f^{-1} T_o) + \frac{C_4}{C_8} I_{out} \ddot{\theta}_{out} \quad (48)$$

Following the argument in Section 4.2.2, we cannot have T_m jump to T_{max} at $t = 0$, as this would imply a jump in T_2 , which would violate any dT_2/dt limitation. Therefore, T_m should be increased gradually from $T_m(0)$ to T_{max} at the beginning of the gearshift. For this proof adaptation however, we neglect the effect of gradually ramping T_m on the synchronization time t_s – we assume the ramp is completed very quickly, so $T_m \approx T_{max}$. Further, we assume that $\dot{\theta}_{out}(t) = \dot{\theta}_{out}(0)$ and $T_o(t) = T_o(0)$ for the duration of the inertia phase, which we also assumed in Theorem 3 by imposing T_2 constant

for the duration of the inertia phase. We now have a linear ordinary differential equation of the same form than in Theorem 3, which we also solve imposing $\dot{\theta}_m(0) = i_2\dot{\theta}_{\text{out}}(0)$. We obtain an adapted condition for the possibility of a no-jerk gearshift as follows

$$\exists t_s > 0 \quad \text{s.t.} \quad 0 = -i_1 \frac{v_i + a_r t_s}{r_w} + \exp\left(-\frac{\gamma c_m}{I_m} t_s\right) i_2 \frac{v_i}{r_w} + \frac{\gamma T_{\text{max}} - \tau}{\gamma c_m} \left[1 - \exp\left(-\frac{\gamma c_m}{I_m} t_s\right)\right] \quad (49)$$

5 Conclusion

In this article, we presented theorems that describe the fundamental limitations to no-jerk gearshift in the presence of motor and clutch saturation. We showed that transmissions with a one-way clutch have stronger limitations than their friction clutch counterparts. This means that a one-way clutch transmission will fail to provide a no-jerk gearshift under a wider set of driving conditions. We also showed that transmissions with a planetary gearset architecture have different dynamics than transmissions with parallel shaft architectures, which requires slight adaptations of the theorems for fundamental limitations of no-jerk gearshifts.

This work has important implications for automotive engineers. The theorems are tools to quickly evaluate if a no-jerk gearshift is possible given a vehicle description, driving scenario, and transmission architecture. This can be used to motivate the choice of a transmission type over another during the conceptual design phase of a new vehicle. Also, the theorems can be integrated in a transmission control unit: when a gearshift is desired, the unit quickly evaluates if a no-jerk gearshift is possible, and then decides if the driving torque should be smoothly reduced prior to initiating the gearshift, or if the gearshift can be initiated with the current DTD without substantial risks of saturating the motor and obtaining a large driveline jerk. This work also has important implications for academic researchers. The theorems present conditions where gearshift jerk is unavoidable, and any attempt at eliminating jerk with a new controller design would be futile. Moreover, this work helps to identify when two transmission architectures are mathematically equivalent, and therefore will result in the same fundamental limitations.

Funding sources

This work was supported by Mitacs and Fonds de recherche Nature et technologies.

References

- [1] K. T. Ulrich and S. D. Eppinger, *Product design and development*, 5th ed. New York: McGraw-Hill/Irwin, 2012.
- [2] G. Pahl, W. Beitz, J. Feldhusen, and K.-H. Grote, *Engineering Design*. London: Springer London, 2007.
- [3] M. J. French, *Conceptual Design for Engineers*. London: Springer London, 1999.
- [4] G. Wu, X. Zhang, and Z. Dong, "Powertrain architectures of electrified vehicles: Review, classification and comparison," *Journal of the Franklin Institute*, vol. 352, no. 2, pp. 425–448, Feb. 2015.

- [5] Y. Yang, K. A. Ali, J. Roeleveld, and A. Emadi, "State-of-the-art electrified powertrains - hybrid, plug-in, and electric vehicles," *International Journal of Powertrains*, vol. 5, no. 1, p. 1, 2016.
- [6] P. E. Resele and O. Bitsche, "Advanced Fully Automatic Two-Speed Transmission for Electric Automobiles," in *SAE Technical Paper*, Aug. 1995.
- [7] Y. Lei, J. Hu, Y. Fu, S. Sun, X. Li, W. Chen, L. Hou, and Y. Zhang, "Control strategy of automated manual transmission based on active synchronisation of driving motor in electric bus," *Advances in Mechanical Engineering*, vol. 11, no. 4, Apr. 2019.
- [8] H. V. Alizadeh and B. Boulet, "Robust control of synchromesh friction in an electric vehicle's clutchless automated manual transmission," in *2014 IEEE Conference on Control Applications (CCA)*, Oct. 2014, pp. 611–616.
- [9] C.-Y. Tseng and C.-H. Yu, "Advanced shifting control of synchronizer mechanisms for clutchless automatic manual transmission in an electric vehicle," *Mechanism and Machine Theory*, vol. 84, pp. 37–56, Feb. 2015.
- [10] F. Amisano, E. Galvagno, M. Velardocchia, and A. Vigliani, "Automated manual transmission with a torque gap filler Part 1: kinematic analysis and dynamic analysis," *Proceedings of the Institution of Mechanical Engineers, Part D: Journal of Automobile Engineering*, vol. 228, no. 11, pp. 1247–1261, Sep. 2014.
- [11] E. Galvagno, M. Velardocchia, and A. Vigliani, "Analysis and simulation of a torque assist automated manual transmission," *Mechanical Systems and Signal Processing*, vol. 25, no. 6, pp. 1877–1886, Aug. 2011.
- [12] A. Sornioti, T. Holdstock, G. L. Pilone, F. Viotto, S. Bertolotto, M. Everitt, R. J. Barnes, B. Stubbs, and M. Westby, "Analysis and simulation of the gearshift methodology for a novel two-speed transmission system for electric powertrains with a central motor," *Proceedings of the Institution of Mechanical Engineers, Part D: Journal of Automobile Engineering*, vol. 226, no. 7, pp. 915–929, Jul. 2012.
- [13] S. Hong, H. Son, S. Lee, J. Park, K. Kim, and H. Kim, "Shift control of a dry-type two-speed dual-clutch transmission for an electric vehicle," *Proceedings of the Institution of Mechanical Engineers, Part D: Journal of Automobile Engineering*, vol. 230, no. 3, pp. 308–321, Feb. 2016.
- [14] B. Gao, Q. Liang, Y. Xiang, L. Guo, and H. Chen, "Gear ratio optimization and shift control of 2-speed I-AMT in electric vehicle," *Mechanical Systems and Signal Processing*, vol. 50-51, pp. 615–631, Jan. 2015.
- [15] M. S. Mousavi, A. Pakniyat, T. Wang, and B. Boulet, "Seamless dual brake transmission for electric vehicles: Design, control and experiment," *Mechanism and Machine Theory*, vol. 94, pp. 96–118, Dec. 2015.
- [16] Y. Tian, J. Ruan, N. Zhang, J. Wu, and P. Walker, "Modelling and control of a novel two-speed transmission for electric vehicles," *Mechanism and Machine Theory*, vol. 127, pp. 13–32, Sep. 2018.

- [17] S. Fang, J. Song, H. Song, Y. Tai, F. Li, and T. Sinh Nguyen, “Design and control of a novel two-speed Uninterrupted Mechanical Transmission for electric vehicles,” *Mechanical Systems and Signal Processing*, vol. 75, pp. 473–493, Jun. 2016.
- [18] M. Roozegar, Y. Setiawan, and J. Angeles, “Design, modelling and estimation of a novel modular multi-speed transmission system for electric vehicles,” *Mechatronics*, vol. 45, pp. 119–129, Aug. 2017.
- [19] S. Murata, “Innovation by in-wheel-motor drive unit,” *Vehicle System Dynamics*, vol. 50, no. 6, pp. 807–830, Jun. 2012.
- [20] Y. Tang, “Control system for an all-wheel drive electric vehicle,” US Patent US7 739 005B1, Jun., 2010.
- [21] —, “Dual motor drive and control system for an electric vehicle,” US Patent US8 453 770B2, Jun., 2013.
- [22] J. Wu, J. Liang, J. Ruan, N. Zhang, and P. D. Walker, “A robust energy management strategy for EVs with dual input power-split transmission,” *Mechanical Systems and Signal Processing*, vol. 111, pp. 442–455, Oct. 2018.
- [23] —, “Efficiency comparison of electric vehicles powertrains with dual motor and single motor input,” *Mechanism and Machine Theory*, vol. 128, pp. 569–585, Oct. 2018.
- [24] M. Hu, J. Zeng, S. Xu, C. Fu, and D. Qin, “Efficiency Study of a Dual-Motor Coupling EV Powertrain,” *IEEE Transactions on Vehicular Technology*, vol. 64, no. 6, pp. 2252–2260, Jun. 2015, conference Name: IEEE Transactions on Vehicular Technology.
- [25] J. Miller, “Hybrid electric vehicle propulsion system architectures of the e-CVT type,” *IEEE Transactions on Power Electronics*, vol. 21, no. 3, pp. 756–767, May 2006.
- [26] A. Sorniotti, T. Holdstock, M. Everitt, M. Fracchia, F. Viotto, C. Cavallino, and S. Bertolotto, “A novel clutchless multiple-speed transmission for electric axles,” *International Journal of Powertrains*, vol. 2, no. 2/3, p. 103, 2013.
- [27] J. Liang, H. Yang, J. Wu, N. Zhang, and P. D. Walker, “Shifting and power sharing control of a novel dual input clutchless transmission for electric vehicles,” *Mechanical Systems and Signal Processing*, vol. 104, pp. 725–743, May 2018.
- [28] F. Bottiglione, S. De Pinto, G. Mantriota, and A. Sorniotti, “Energy Consumption of a Battery Electric Vehicle with Infinitely Variable Transmission,” *Energies*, vol. 7, no. 12, pp. 8317–8337, Dec. 2014.
- [29] A. Sorniotti, S. Subramanyan, A. Turner, C. Cavallino, F. Viotto, and S. Bertolotto, “Selection of the Optimal Gearbox Layout for an Electric Vehicle,” *SAE International Journal of Engines*, vol. 4, no. 1, pp. 1267–1280, Apr. 2011.
- [30] M. Golkani, M. Steinberger, M. Bachinger, J. Rumetshofer, M. Stolz, and M. Horn, “Optimal Gear Shift Strategy for Dual Clutch Transmissions,” *IFAC-PapersOnLine*, vol. 50, no. 1, pp. 4800–4805, Jul. 2017.

- [31] J. Ye, K. Zhao, Y. Liu, X. Huang, and H. Lin, “Multi-stage global trajectory optimization for the overlapping shift of a seamless two-speed transmission using Legendre pseudo-spectral method,” *Advances in Mechanical Engineering*, vol. 9, no. 12, Dec. 2017.
- [32] A. Haj-Fraj and F. Pfeiffer, “Optimal control of gear shift operations in automatic transmissions,” *Journal of the Franklin Institute*, vol. 338, no. 2-3, pp. 371–390, Mar. 2001.
- [33] P. Walker, B. Zhu, and N. Zhang, “Powertrain dynamics and control of a two speed dual clutch transmission for electric vehicles,” *Mechanical Systems and Signal Processing*, vol. 85, pp. 1–15, Feb. 2017.
- [34] B. Gao, Y. Xiang, H. Chen, Q. Liang, and L. Guo, “Optimal Trajectory Planning of Motor Torque and Clutch Slip Speed for Gear Shift of a Two-Speed Electric Vehicle,” *Journal of Dynamic Systems, Measurement, and Control*, vol. 137, no. 6, p. 061016, Jun. 2015.
- [35] S. Kim, J. Oh, and S. Choi, “Gear shift control of a dual-clutch transmission using optimal control allocation,” *Mechanism and Machine Theory*, vol. 113, pp. 109–125, Jul. 2017.
- [36] T. Holdstock, A. Sorniotti, N. Suryanto, L. Shead, F. Viotto, C. Cavallino, and S. Bertolotto, “Linear and non-linear methods to analyse the drivability of a through-the-road parallel hybrid electric vehicle,” *International Journal of Powertrains*, vol. 2, no. 1, p. 52, 2013.
- [37] O. H. Dagci, H. Peng, and J. W. Grizzle, “Hybrid Electric Powertrain Design Methodology With Planetary Gear Sets for Performance and Fuel Economy,” *IEEE Access*, vol. 6, pp. 9585–9602, 2018.
- [38] J. Liu, L. Yu, Q. Zeng, and Q. Li, “Synthesis of multi-row and multi-speed planetary gear mechanism for automatic transmission,” *Mechanism and Machine Theory*, vol. 128, pp. 616–627, Oct. 2018.
- [39] A. E. Bayrak, Y. Ren, and P. Y. Papalambros, “Topology Generation for Hybrid Electric Vehicle Architecture Design,” *Journal of Mechanical Design*, vol. 138, no. 8, p. 081401, Aug. 2016.
- [40] S. Bai, J. Maguire, and H. Peng, *Dynamic analysis and control system design of automatic transmissions*. Warrendale, PA, USA: Society of Automotive Engineers, 2013.
- [41] J. Goss, R. Wrobel, P. Mellor, and D. Staton, “The design of AC permanent magnet motors for electric vehicles: A design methodology,” in *2013 International Electric Machines & Drives Conference*. Chicago, IL, USA: IEEE, May 2013, pp. 871–878.